Design Consideration and Conductor Selection of A Low AC Loss HTS REBCO Magnet Carrying High Currents at 20 K and 40 K

Honghai Song, *Senior Member, IEEE,* Zhenan Jiang, *Senior Member, IEEE,* and Wenjuan Song, *Member, IEEE*

***Abstract*— AC loss in high temperature superconductor coils have been frequently studied, however, mostly for AC power applications at 77 K, rather than specifically for high current but low frequency AC superconducting magnet at 20-40 K. Due to their easy operation and Helium shortage, more HTS magnet systems employ conduction-cooling with cryocoolers. The HTS magnets are known for high stability and likely tolerate high AC loss, but it is unclear what is the maximum AC frequency assuming that cryocooler has limited capability (a few hundred Watts) for the 20-40 K temperature range. This paper will specifically study AC loss in a simple HTS dipole but with three conductor/cable options using simulations, (1) 12 mm wide tape, (2) two parallel 6 mm wide tapes, and (3) 6/2 (six 2 mm strands) Roebel cables. It has been found that the magnet at 5 Hz generates 200 – 400 W AC loss at 20 K or 40 K, potentially be cooled by two single stage cryocoolers. The 6/2 Roebel cable based magnet may allow higher frequency (6-8 Hz) due to its transposition and narrower conductor width.**

***Index Terms*— AC Loss, Conduction Cooling, HTS Cable, HTS Magnet, Roebel Cable.**

I. Introduction

Great progress has been made in REBCO tapes (where RE stands for Rare-Earth, B is for Barium, C is for Copper and O is for Oxygen) in both high critical current I_c owing to new flux pinning doping and long-length production due to process improvement. Nearly a dozen of REBCO manufactures worldwide are producing high quality REBCO conductors. With more conductor available, more HTS magnet prototypes have been successfully demonstrated for high field applications. HTS magnet has been known for high thermal and electrical stability, and a few low frequency or fast-ramping rate HTS magnets have been developed [1]–[3]. Another type of AC magnet application is the horizontal or vertical scanning for proton cancer therapy [4]. Such scanning magnets are currently made of Cu cable with water-cooling and operate in a frequency range of 1-25 Hz. It will not only consume high electrical power but also require complex of chilly water system. Given that the frequency is not very high and HTS has large thermal margin, it seems promising to design such scanning magnet with REBCO conductors.

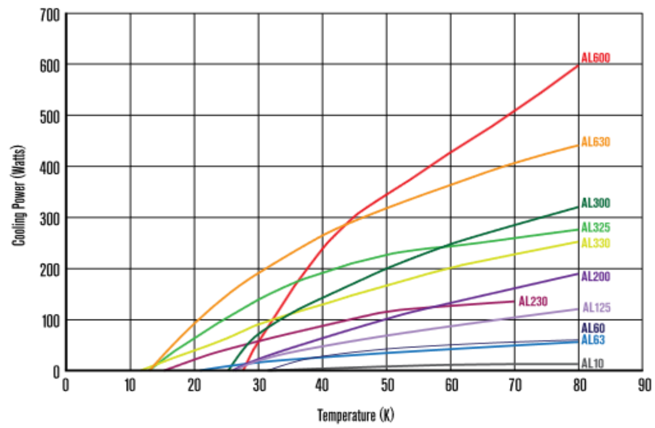

Fig. 1. Cooling power capacity of various CryoMech cryocoolers. For example, a single cryocooler has maximum cooling power of 100 W at 20 K and 270 W at 40 K.

Possible operation of HTS magnet at higher temperature (for instance 20 K – 40 K) other than 4.2 K [5], allows higher heat capacity and even Cu thermal conductivity. Moreover, due to easy operation and Helium shortage [6], conduction-cooling with cryocoolers becomes a more effective method for HTS magnets [7]–[11]. However, using cryocoolers is limited by its own capacity and its related infrastructure cost. Usually, a HTS magnet may be equipped with cryocoolers. Based on Cryomech's cryocoolers specifications [12], a single cryocooler has maximum cooling power of 100 W at 20 K, and 270 W at 40K as shown in Fig. 1. In addition to thermal loads include current leads, the radiation loss, suspension links and ramp loss [13]. The AC superconducting magnet will have not only general thermal loads including current leads, radiation loss and ramp-up and down hysteresis loss, but also outstanding AC loss due to AC operation currents[14]. It's important to estimate the total loss so that it may be cooled a limited number of cryocooler.

Manuscript receipt and acceptance dates will be inserted here. This work was supported in part by 2019-2024 US DOE Ernest Courant Traineeship in Accelerator Sciences and Engineering, the educational program of next generation of accelerator physicists and engineer, US Department of Energy, DE-SC0020375, and New Zealand Ministry of Business, Innovation and Employment (MBIE) by the Strategic Science Investment Fund ''Advanced Energy Technology Platforms'' under Contract RTVU2004. *(Corresponding author: Honghai Song)*

H. Song is with the State University of New York at Stony Brook, New York, 11733, USA (e-mail: honghaisong@gmail.com).

Z. Jiang is with Robinson Research Institute, Victoria University of Wellington,6140 New Zealand (e-mail: zhenan.jiang@vuw.ac.nz).

W. Song is with James Watt School of Engineering, University of Glasgow, Glasgow, G12 8QQ, UK, (e-mail:wenjuan.song@glasgow.ac.uk).

Color versions of one or more of the figures in this paper are available online at http://ieeexplore.ieee.org.

Digital Object Identifier will be inserted here upon acceptance.

There have been numerous publications on AC loss simulations and experiments in HTS coils [15]–[23]. However, majority of AC loss data stay at a temperature range between 77 K – 65 K and lower currents (<100 A) though with higher frequency of 100 – 10k Hz. Less studies have been conducted for HTS low frequency AC magnets at 20 K – 40 K temperatures with high currents (300 - 400 A) and at low frequency 1 – 25 Hz [24]–[27].

Moreover, various methods have been studied to reduce AC loss in HTS coils by replacing a tape with a stack of narrower tapes[28] or Roebel cables [29]–[33], tuning turn-to-turn spacing, grading I_c for the center winding and end windings, and adding flux diverter at the coil ends [34], [35]. H formulation based FEM method has been used in the AC loss computation [36]–[43]. Here, a simple dipole HTS magnet system for a 0.5 T scanning magnet with approximately 1.5 T peak field, has been designed using three different conductor/cable options. Their AC loss will be calculated to study the AC loss dependence of conduction selection. Their AC loss will be further evaluated against allowable cooling power provided by available cryocoolers. Given the operation current I_{op} stays the same, I_c of conductor/cable will decrease with temperature increasing from 20 K to 40 K. As a result, ratio of I_{op}/I_c will increase, so their AC loss will increase. But the question is if the increase in cooling power will balance the AC loss increase.

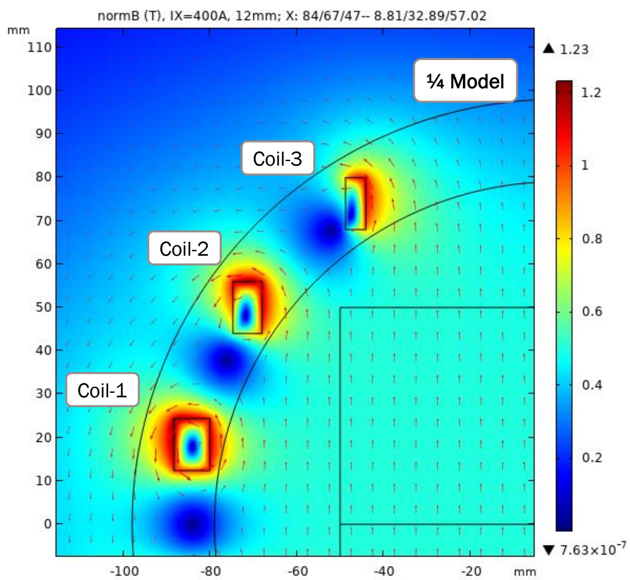

Fig. 2. A ¼ model of the HTS dipole, with 3 coils on the upper. Applied current is about 400 A, max field is about 1.5 T in the coil winding pack. It has 12 mm wide tapes, and coil-1, 2 and 3 have turns number of 84, 67 and 47.

II. A simple HTS dipole

A simple HTS dipole which has 6 sets of racetracks (3 in the upper and 3 in the lower) is being modeled for AC loss computation with the three conductor/cable options, as shown in Fig. 2. The model is not to scale, but its average current density intends to follow the cos(Θ) pattern, to achieve 0.1% field homogeneity with an aperture size of 10 cm. Fig.1 shows ¼ of the magnet cross section. The three coils are named coil-1, coil-2, and coil-3 from the median plane to the top. Their specifications are listed in Table I, which have turn #, coil cross-sections (vertical height and horizontal width), and inner-lower corner locations.

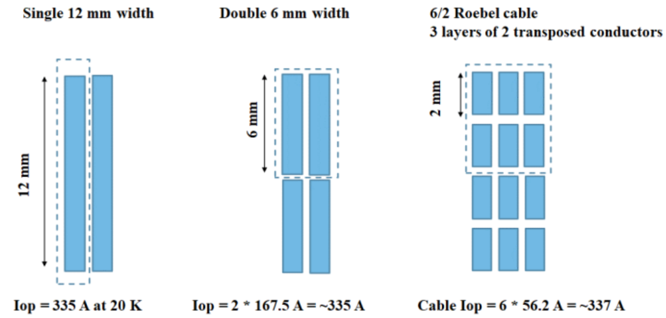

Fig. 3. Three conductor and cable options, 12 mm wide, two parallel 6 mm, and 6/2 Roebel cable. The dashed rectangle indicates the minimum cell size which has similar transport currents at around 336 A. The 12 mm and 6 mm width have identical radial build, while the Roebel based one will have 1.5 times thicker radial build.

TABLE I
HTS Dipole Magnetic Specifications

Coil-#	Turns#	Coil Height in Y(mm)	Coil Thickness in X (mm)	Inner corner location (X,Y) in mm
Coil-1	84	12	8.4	(-80.0, 12.4)
Coil-2	67	12	6.7	(-68.0, 44.0)
Coil-3	47	12	4.7	(-44.1,68.0)

TABLE II
AC loss of the HTS dipole at **20 K** for three cases of conductor/cable cases

Conductor/cable selection	Single 12 mm	Two parallel 6 mm	Roebel cable 6/2
I_{op} (A)	335	335	337
Coil B_{max} (T)	1.5	1.5	~1.5
Conductor/cable I_c(1.5 T and 20K)	3000	3000	3000
¼ AC loss (J/m/cycle)	8.1	8.33	6.33
Total AC loss (J/m/cycle)	32.4	33.32	25.32

AC loss of such a dipole system made of three conductions/cables will be calculated and compared. They are (1) 12 mm wide tape, (2) two parallel 6 mm tape, and (3) equivalent 6/2 Roebel cable. Transposition pitch of the Roebel cable is 90 mm. The dipole center field is required at 0.5 T by the 6 coils, so the required operation current is 335 A for a single 12 mm wide conductor, and about 335 A for the two parallel 6 mm tapes, and 337 A for the equivalent Roebel cable 6/2. Namely, the Roebel cable has six 2 mm strands in total. The details of simulation method can be found form reference [34]. Conductor $I_c(B, T)$ is based on SuperPower conductor specs [44] and employs fitting function as mentioned in [34]. The 12 mm tape has about 3000 A at 1.5 T and 20 K, and about 1500 A at 1.5 T and 40 K. The relevant specifications have been summarized in Table II. If the magnet scanning frequency is 1 Hz, the HTS coil winding pack will experience 3 T/s field changing rate. If 10 Hz, it will be 30 T/s.

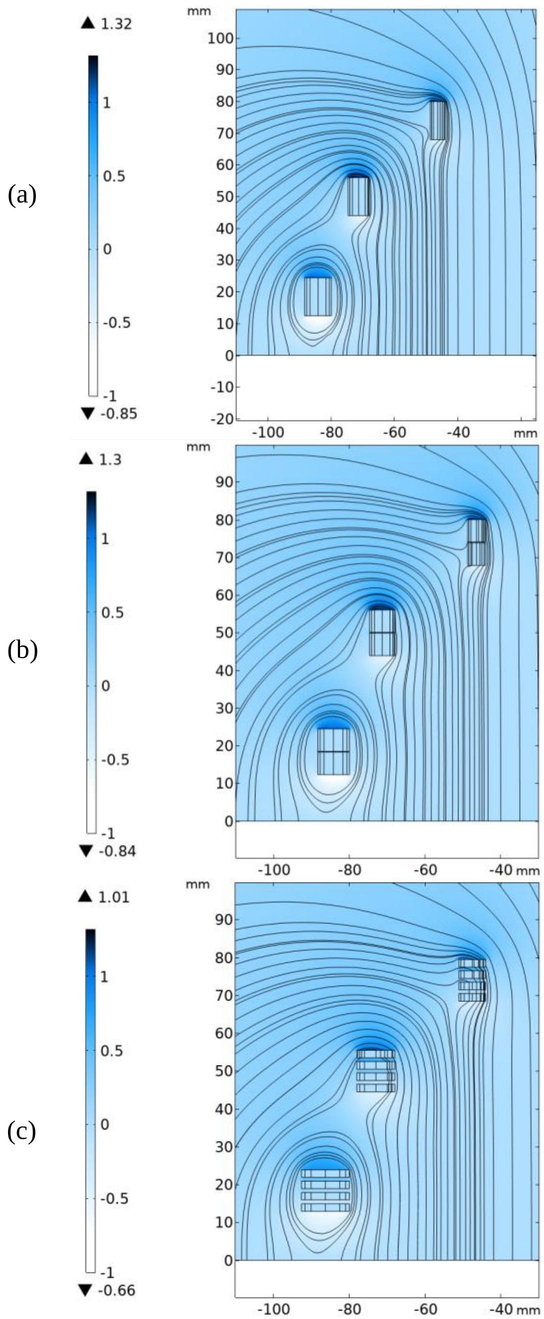

Fig. 4. The perpendicular field of the ¼ dipole cross-section including the three coils (1-3). From top to bottom, they are made of three conductor cases. (a): 12 mm wide conductor, (b): two parallel 6 mm wide conductor, (c) Roebel cable 6/2.

III. Results and Analysis

The magnet wound with the 12 mm single tape will result in single pancake coils; that wound with the two parallel 6 mm will result in double pancake coils; that wound with the 6/2 will be equivalent to a stack of two double-pancake coils. Because the 6/2 Roebel cable has three layers of transposed 2 mm strands, and its single cable thickness is 0.3 mm, so that the total coil radial thickness is 1.5 times of the other two cases.

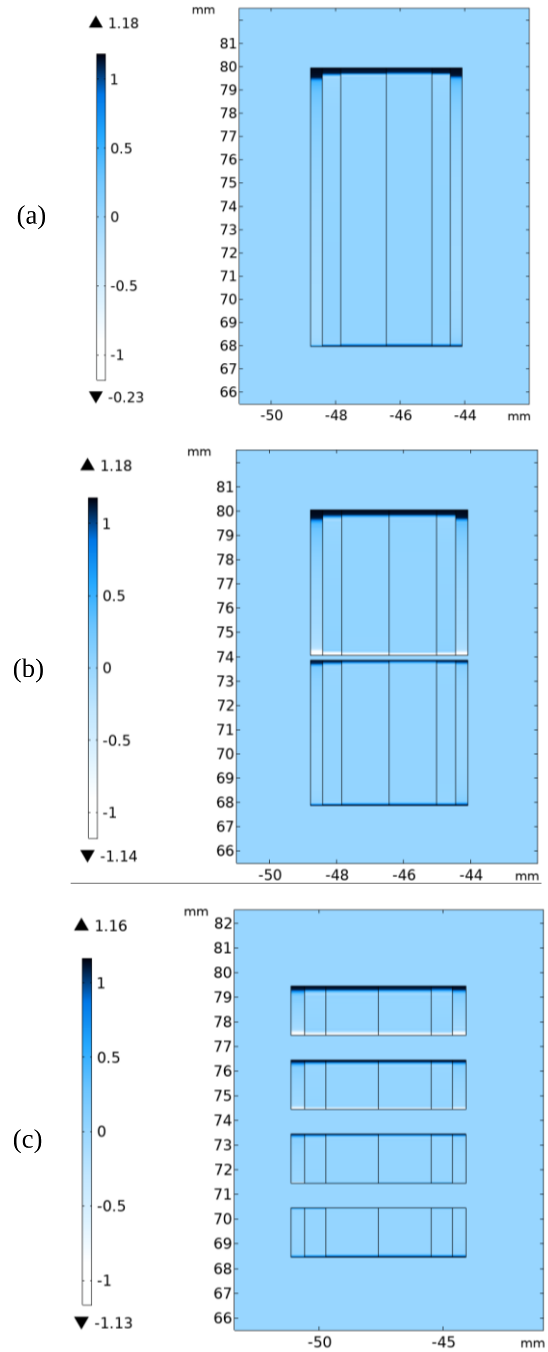

Fig. 5. The induced current density J/Jc in the coil-3 cross-section for the three conductor cases. (a): 12 mm wide conductor, (b): two parallel 6 mm wide conductor, (c) Roebel cable 6/2. Dark and light color currents are in opposite directions. and the applied frequency is 25 Hz.

Table III lists details of the simulation and the simulation result. The ¼ AC loss values in the magnets wound with the single 12 mm tape, two 6 mm parallel tapes, and the Roebel 6/2 cable, are 8.1 J/m/cycle, 8.33 J/m/cycle and 6.33 J/m/cycle, respectively. For the whole HTS dipole system, the AC loss number will be 4 times of the numbers shown in the above. There is almost no difference in the AC loss values in the magnets wound with the single 12 mm and two parallel 6 mm conductors. However, the result shows 25% AC loss reduction by employing the 6/2 Roebel cable.

Fig. 4 displays the perpendicular magnetic component of the magnetic field ($B_\perp$) and magnetic streamlines around the magnets made of the three conductor/cable. The magnets wound with the 12 mm wide tapes and two parallel 6 mm tapes have almost the same the $B_\perp$ distributions and magnetic streamlines around the magnets. This can explain the very similar AC loss values for the first two cases shown in Table II because the AC loss in the magnets is governed by $B_\perp$ components of the coils. In addition, the maximum $B_\perp$ values for the two cases are very similar (1.32 T and 1.3 T), which also indirectly supports the similar AC loss result mentioned above. The magnet wound with the 6/2 Roebel cable has less $B_\perp$ values around the coils and the maximum $B_\perp$ value (1.01 T) compared to the two cases. This explains the low AC loss values of the magnet compared with the other two magnets.

Fig. 5 shows the J/J_c distributions of coil-3 in the magnets and the applied frequency is 25 Hz. The coil-3 was chosen on the base of the strongest magnetic field it experiences due to the superposition of the magnetic fields generated from the coil-1 and coil-2. The region where $|J/J_c| > 1$ represents magnetic field penetration and AC loss is generated in the penetrated region. When wound with the 12 mm wide tape, as shown in Fig. 5(a), field penetration mainly occurs in the upper part of coil-3. However, when wound with the two parallel 6 mm tapes and 6/2 Roebel cable, there is visible shielding currents inside the upper pancake coil(s) of coil-3. In the Roebel case, the upper pancake coil is equivalent to two pancake coils or a double pancake coil. The opposite current directions (dark vs light color in the figure) in the coils indicates the loss mechanism in the upper pancake coils is magnetization loss. Because magnetization loss is proportional to the conductor width and hence the AC loss value in the upper pancake coil wound with the 6/2 Roebel cable is lower than that wound with the two parallel 6 mm tapes. In the lower pancake coils of the two cases, there is nearly no shielding current for both cases. However, between them, there is more field penetration in the case of using the two parallel 6 mm tapes. Similar tendency is obtained in coil-1 and coil-2 and this explains why the magnet wound with the Roebel cable gives the smallest AC loss than the other two options.

TABLE III
FREQUENCY DEPENDENCE OF TOTAL AC LOSS (J) OF THE HTS DIPOLE AT **20 K** FOR THREE CASES OF CONDUCTOR/CABLE CASES.

Frequency (Hz)	Single 12 mm {J}	Two parallel 6 mm (J)	Roebel cable 6/2 (J)
1	32.4	33.32	25.32
2	64.8	66.64	50.64
4	129.6	133.28	101.28
6	194.4	199.92	151.92
8	259.2	266.56	202.56
10	324	333.2	253.2

Given that the HTS magnet operates in the frequency range of 1 – 10 Hz and the AC loss per cycle is constant, the total AC losses is proportional to the frequency. Table II shows dependence of total AC losses (J) values on frequencies from 1 to 10 Hz. It is worth noting there is slightly non-linear AC loss dependence on frequency due to *E*-*J* power law. As mentioned in the introduction, the maximum conduction cooling capacity of one of the best cooling CryoMech cryocoolers is 100 W at 20 K. With that, the magnets wound with the single 12 mm and the two parallel 6 mm can only operate at max 2 Hz, and the magnet wound with the Roebel 6/2 can still function at 6 Hz. With two cryocoolers, the total cooling power becomes 200 W. In this case, the first two cases can run up to 6 Hz, while the Roebel cable case can be operated at 8 Hz.

Since the single cryocooler cooling power increases from 100 W at 20 K to 270 W at 40 K, one may consider elevate the HTS magnet temperature from 20 K to 40 K. Table IV and V will list the detail numbers at 40 K.

TABLE IV
AC LOSS OF THE HTS DIPOLE AT **40 K** FOR THREE CASES OF CONDUCTOR/CABLE CASES

Conductor/cable selection	Single 12 mm	Two parallel 6 mm	Roebel cable 6/2
I_{op} (A)	335	335	337
Coil B_{max} (T)	1.5	1.5	~1.5
Conductor/cable I_c(1.5 T and 40K)	1500	1500	1500
¼ AC loss (J/m/cycle)	19.94	19.96	14.76
Total AC loss (J/m/cycle)	79.76	79.84	59.04

TABLE V
FREQUENCY DEPENDENCE OF AC LOSS OF THE HTS DIPOLE AT **40 K** FOR THREE CASES OF CONDUCTOR/CABLE CASES

Frequency (Hz)	Single 12 mm (W)	Two parallel 6 mm (W)	Roebel cable 6/2 (W)
1	79.76	79.84	59.04
2	159.52	159.68	118.08
4	319.04	319.36	236.16
6	478.56	479.04	354.24
8	638.08	638.72	472.32
10	797.6	798.4	590.4

In this comparison between 20 K and 40 K, the HTS magnet has the same 0.5 T center field, which means that the magnet operation current I_{op} stay the same. But the I_c(1.5 T) decreases as temperature increases from 3000 A at 20 K to

~1500 A at 40 K. Accordingly, the ratio $I_{op}/I_c(1.5\ T)$ has changed from ~11% to ~ 22%.

Higher I_{op}/I_c ration will result in higher AC loss per former studies. The higher AC loss at 40 K is about 2.5 times, 2.4 time, and 2.3 times than that of them at 20 K, for the three cases of conductor respectively.

Based on Table V, if with two cryocooler, max cooling power is 540 W, so that the single 12 mm or double 6 mm based magnets may operate at 6 Hz where it has about 478 W, but the Roebel based magnet may operate at 8 Hz where it has about 472 W. Beyond the threshold frequencies, the AC loss is too large to be cooled.

IV. Conclusion

A simple 0.5 T HTS magnet system which intends to operate in the frequency range of 1 Hz to 10 Hz have been studied with 2D FEM model based on H-Formulation. Three conductor/cable options, (1) single 12mm, (2) parallel 6 mm and (3) the Roebel 6/2 are considered in the coil winding. Their AC loss has been evaluated against available cooling power.

The magnet wound with the single 12 mm has similar AC loss to that wound with the two 6 mm in parallel. At 20K, the Roebel cable - based magnet will have 25% reduction in its AC loss. Given that the large AC can be removed by the available cryocoolers, the HTS magnet made of the first two cases allow to operate at only 4 Hz, while the Roebel based magnet may operate at 6 Hz, where the AC loss can be cooled by the available cryocoolers.

With the same operating current I_{op} = 335 A, which is 11% of I_c at 1.5 T and 20 K and 22% of I_c at 1.5 T and 40 K, the magnet may tolerate higher frequency up to 8 Hz at 40 K for the Roebel cable case. The increased cooling power can cover the increased AC loss while temperature changed from 20 K to 40 K. Note that the I_{op} / I_c ratio is kept low, this conclusion is just a reference and might not apply to other HTS magnet. Detailed computation is needed for a specific HTS magnet including conductor, operating current or temperature margin.

References

[1] H. Piekarz, S. Hays, J. Blowers, B. Claypool, and V. Shiltsev, "Record fast-cycling accelerator magnet based on HTS conductor," *Nucl. Instrum. Methods Phys. Res. Sect. Accel. Spectrometers Detect. Assoc. Equip.*, vol. 943, p. 162490, Nov. 2019, doi: 10.1016/j.nima.2019.162490.

[2] H. Piekarz, S. Hays, B. Claypool, M. Kufer, and V. Shiltsev, "Record High Ramping Rates in HTS Based Superconducting Accelerator Magnet," *IEEE Trans. Appl. Supercond.*, vol. 32, no. 6, pp. 1–4, Sep. 2022, doi: 10.1109/TASC.2022.3151047.

[3] I. Park, C. Lee, J. Park, S. Kim, and S. Jeong, "Performance of the Fast-Ramping High Temperature Superconducting Magnet System for an Active Magnetic Regenerator," *IEEE Trans. Appl. Supercond.*, vol. 27, no. 4, pp. 1–5, Jun. 2017, doi: 10.1109/TASC.2017.2652324.

[4] V. Anferov, "Combined X–Y scanning magnet for conformal proton radiation therapy," *Med. Phys.*, vol. 32, no. 3, pp. 815–818, 2005, doi: 10.1118/1.1862801.

[5] H. Song, K. Gagnon, and J. Schwartz, "Quench behavior of conduction-cooled Y Ba2Cu3O7−δ coated conductor pancake coils stabilized with brass or copper," *Supercond. Sci. Technol.*, vol. 23, no. 6, p. 065021, May 2010, doi: 10.1088/0953-2048/23/6/065021.

[6] D. Danabalan *et al.*, "The principles of helium exploration," *Pet. Geosci.*, vol. 28, no. 2, p. petgeo2021, May 2022, doi: 10.1144/petgeo2021-029.

[7] S. Takayama *et al.*, "Design of Conduction-cooled HTS Coils for a Rotating Gantry," *Phys. Procedia*, vol. 67, pp. 879–884, Jan. 2015, doi: 10.1016/j.phpro.2015.06.148.

[8] J. Barkas, Y. Zhai, and M. Safabakhsh, "A cryostat for a 6 T conduction-cooled, no-insulation multi-pancake HTS solenoid," *IOP Conf. Ser. Mater. Sci. Eng.*, vol. 1240, no. 1, p. 012142, May 2022, doi: 10.1088/1757-899X/1240/1/012142.

[9] Y. Zhai, C. Niu, X. Liu, F. Wang, J. Liu, and Q. Wang, "Conduction-Coolled HTS Magnets Closed-Loop System Excited by a Rotating Magnets Flux Pump," *IEEE Trans. Appl. Supercond.*, vol. 32, no. 6, pp. 1–5, Sep. 2022, doi: 10.1109/TASC.2022.3157253.

[10] H. Maeda and Y. Yanagisawa, "Recent Developments in High-Temperature Superconducting Magnet Technology (Review)," *IEEE Trans. Appl. Supercond.*, vol. 24, no. 3, pp. 1–12, Jun. 2014, doi: 10.1109/TASC.2013.2287707.

[11] S. Awaji *et al.*, "AC Losses of an HTS Insert in a 25-T Cryogen-Free Superconducting Magnet," *IEEE Trans. Appl. Supercond.*, vol. 25, no. 3, pp. 1–5, Jun. 2015, doi: 10.1109/TASC.2014.2366552.

[12] "Comparison Chart," *Cryomech*. https://www.cryomech.com/comparison-chart/ (accessed Nov. 13, 2022).

[13] Y. Iwasa, *Case studies in superconducting magnets: design and operational issues*, Second edition. New York: Springer, 2009.

[14] M. Breschi *et al.*, "AC Losses in the First ITER CS Module Tests: Experimental Results and Comparison to Analytical Models," *IEEE Trans. Appl. Supercond.*, vol. 31, no. 5, pp. 1–5, Aug. 2021, doi: 10.1109/TASC.2021.3061950.

[15] E. Pardo, J. Šouc, and J. Kováč, "AC loss in ReBCO pancake coils and stacks of them: modelling and measurement," *Supercond. Sci. Technol.*, vol. 25, no. 3, p. 035003, Mar. 2012, doi: 10.1088/0953-2048/25/3/035003.

[16] G. Liu, G. Zhang, and L. Jing, "Experimental and numerical study of the frequency-dependent transport ac losses of the $YBa_2Cu_3O_{7-\delta}$ coil with and without flux diverters," *Supercond. Sci. Technol.*, vol. 32, no. 5, p. 055002, May 2019, doi: 10.1088/1361-6668/ab014f.

[17] Z. Jiang, W. Song, X. Pei, J. Fang, R. A. Badcock, and S. C. Wimbush, "15% reduction in AC loss of a 3-phase 1 MVA HTS transformer by exploiting asymmetric conductor critical current," *J. Phys. Commun.*, vol. 5, no. 2, p. 025003, Feb. 2021, doi: 10.1088/2399-6528/abe036.

[18] Z. Jiang *et al.*, "AC loss measurements in HTS coil assemblies with hybrid coil structures," *Supercond. Sci. Technol.*, vol. 29, no. 9, p. 095011, Jul. 2016, doi: 10.1088/0953-2048/29/9/095011.

[19] Z. Jiang *et al.*, "AC Loss Measurements in a Hybrid REBCO/BSCCO Coil Assembly," *IEEE Trans. Appl. Supercond.*, vol. 27, no. 6, pp. 1–7, Sep. 2017, doi: 10.1109/TASC.2017.2721978.

[20] M. Zhang, W. Yuan, J. Kvitkovic, and S. Pamidi, "Total AC loss study of 2G HTS coils for fully HTS machine applications," *Supercond. Sci. Technol.*, vol. 28, no. 11, p. 115011, Nov. 2015, doi: 10.1088/0953-2048/28/11/115011.

[21] F. Gömöry *et al.*, "AC Loss in Pancake Coil Made From 12 mm Wide REBCO Tape," *IEEE Trans. Appl. Supercond.*, vol. 23, no. 3, pp. 5900406–5900406, Jun. 2013, doi: 10.1109/TASC.2013.2238986.

[22] D. N. Nguyen, C. H. Kim, J. H. Kim, S. Pamidi, and S. P. Ashworth, "Electrical measurements of AC losses in high temperature superconducting coils at variable temperatures," *Supercond. Sci. Technol.*, vol. 26, no. 9, p. 095001, Sep. 2013, doi: 10.1088/0953-2048/26/9/095001.

[23] M. D. Ainslie, W. Yuan, and T. J. Flack, "Numerical Analysis of AC Loss Reduction in HTS Superconducting Coils Using Magnetic Materials to Divert Flux," *IEEE Trans. Appl. Supercond.*, vol. 23, no. 3, pp. 4700104–4700104, Jun. 2013, doi: 10.1109/TASC.2012.2227639.

[24] J. Kováč *et al.*, "Measurement of AC loss down to 25 K in a REBCO racetrack coil for electrical aircraft motor," *Sci. Rep.*, vol. 12, no. 1, Art. no. 1, Sep. 2022, doi: 10.1038/s41598-022-20625-6.

[25] F. Gomory, S. Takacs, A. Werner, and M. Sochor, "Theoretical Estimation of Electromagnetic Loss From the Movement of Superconducting Coil in the W7-X Stellarator," *IEEE Trans. Appl. Supercond.*, vol. 16, no. 2, pp. 123–126, 2006, doi: 10.1109/TASC.2005.864264.

[26] F. Grilli, V. Zermeño, M. Vojenčiak, E. Pardo, A. Kario, and W. Goldacker, "AC Losses of Pancake Coils Made of Roebel Cable," *IEEE*

Trans. Appl. Supercond., vol. 23, no. 3, pp. 5900205–5900205, Jun. 2013, doi: 10.1109/TASC.2013.2238987.
[27] J. Šouc, E. Pardo, M. Vojenčiak, and F. Gömöry, "Theoretical and experimental study of AC loss in high temperature superconductor single pancake coils," *Supercond. Sci. Technol.*, vol. 22, no. 1, p. 015006, Nov. 2008, doi: 10.1088/0953-2048/22/1/015006.
[28] D. Uglietti, R. Kang, R. Wesche, and F. Grilli, "Non-twisted stacks of coated conductors for magnets: Analysis of inductance and AC losses," *Cryogenics*, vol. 110, p. 103118, Sep. 2020, doi: 10.1016/j.cryogenics.2020.103118.
[29] L. Hao *et al.*, "Conceptual Design and Optimisation of HTS Roebel Tapes," *IEEE Trans. Appl. Supercond.*, vol. 32, no. 4, pp. 1–5, Jun. 2022, doi: 10.1109/TASC.2022.3140712.
[30] Q. Zhang, Y. Yang, and L. Cavallucci, "Performance and Quench Characteristics of a Pancake Coil Wound With the 2G YBCO Roebel Cable," *IEEE Trans. Appl. Supercond.*, vol. 28, no. 4, pp. 1–5, Jun. 2018, doi: 10.1109/TASC.2018.2799140.
[31] R. A. H. de Oliveira, J. M. Pina, W. T. B. de Sousa, R. Nast, A. G. Pronto, and N. Vilhena, "Optimized Shape of Short-Circuited HTS Coils by Cutting Process for Superconducting Fault Current Limiters," *IEEE Trans. Appl. Supercond.*, vol. 31, no. 9, pp. 1–9, Dec. 2021, doi: 10.1109/TASC.2021.3118920.
[32] N. Amemiya, T. Tsukamoto, M. Nii, T. Komeda, T. Nakamura, and Z. Jiang, "Alternating current loss characteristics of a Roebel cable consisting of coated conductors and a three-dimensional structure," *Supercond. Sci. Technol.*, vol. 27, no. 3, p. 035007, Mar. 2014, doi: 10.1088/0953-2048/27/3/035007.
[33] Z. Jiang *et al.*, "Transport AC loss characteristics of a nine strand YBCO Roebel cable," *Supercond. Sci. Technol.*, vol. 23, no. 2, p. 025028, Jan. 2010, doi: 10.1088/0953-2048/23/2/025028.
[34] Z. Jiang, H. Song, W. Song, and R. A. Badcock, "Optimizing coil configurations for AC loss reduction in REBCO HTS fast-ramping magnets at cryogenic temperatures," *Superconductivity*, vol. 3, p. 100024, Sep. 2022, doi: 10.1016/j.supcon.2022.100024.
[35] W. Song, Z. Jiang, M. Staines, S. Wimbush, R. Badcock, and J. Fang, "AC Loss Calculation on a 6.5 MVA/25 kV HTS Traction Transformer With Hybrid Winding Structure," *IEEE Trans. Appl. Supercond.*, vol. 30, no. 4, pp. 1–5, Jun. 2020, doi: 10.1109/TASC.2020.2975771.
[36] B. Shen, F. Grilli, and T. Coombs, "Review of the AC loss computation for HTS using H formulation," *Supercond. Sci. Technol.*, vol. 33, no. 3, p. 033002, Feb. 2020, doi: 10.1088/1361-6668/ab66e8.
[37] Z. Jiang *et al.*, "Exploiting asymmetric wire critical current for the reduction of AC loss in HTS coil windings," *J. Phys. Commun.*, vol. 3, no. 9, p. 095017, Sep. 2019, doi: 10.1088/2399-6528/ab4437.
[38] F. Weng, M. Zhang, T. Lan, Y. Wang, and W. Yuan, "Fully superconducting machine for electric aircraft propulsion: study of AC loss for HTS stator," *Supercond. Sci. Technol.*, vol. 33, no. 10, p. 104002, Aug. 2020, doi: 10.1088/1361-6668/ab9687.
[39] B. J. H. de Bruyn, J. W. Jansen, and E. A. Lomonova, "AC losses in HTS coils for high-frequency and non-sinusoidal currents," *Supercond. Sci. Technol.*, vol. 30, no. 9, p. 095006, Aug. 2017, doi: 10.1088/1361-6668/aa7c74.
[40] Y. Li, Z. Jiang, G. Sidorov, R. Koraua, Y. Sogabe, and N. Amemiya, "AC Loss Measurement in HTS Coil Windings Coupled With Iron Core," *IEEE Trans. Appl. Supercond.*, vol. 29, no. 5, pp. 1–5, Aug. 2019, doi: 10.1109/TASC.2019.2901963.
[41] V. M. R. Zermeño and F. Grilli, "3D modeling and simulation of 2G HTS stacks and coils," *Supercond. Sci. Technol.*, vol. 27, no. 4, p. 044025, Apr. 2014, doi: 10.1088/0953-2048/27/4/044025.
[42] W. Song *et al.*, "AC loss simulation in a HTS 3-Phase 1 MVA transformer using H formulation," *Cryogenics*, vol. 94, pp. 14–21, Sep. 2018, doi: 10.1016/j.cryogenics.2018.07.003.
[43] M. D. Ainslie, V. M. Rodriguez-Zermeno, Z. Hong, W. Yuan, T. J. Flack, and T. A. Coombs, "An improved FEM model for computing transport AC loss in coils made of RABiTS YBCO coated conductors for electric machines," *Supercond. Sci. Technol.*, vol. 24, no. 4, p. 045005, Apr. 2011, doi: 10.1088/0953-2048/24/4/045005.
[44] "Robinson HTS Wire Critical Current Database." https://htsdb.wimbush.eu/ (accessed Nov. 13, 2022).